

Internship from the 22nd of April to the 22nd of July, 2013  
at the Manchester Centre for Nonlinear Dynamics, the University of Manchester.

---

# Particle size segregation in granular free-surface flows

---

**Intern:** Nicolas Macé

**Internship supervisor:** Nico Gray

## Abstract

In granular flows, large particles tend to go at the flow surface, while small particles tend to go at the flow base. This particle size segregation is still poorly understood, especially in natural debris flows, where this effect is combined with strong sheer rates to cause lateral levees formation and flow channelisation.

We seek to model and understand the properties of such granular flows. We base our analysis on large-scale granular chute experiments conducted in 2011 [4]. We model the two-dimensional flow in the centre plane of the avalanche, and we propose and explanation for the observed structure. We develop a code to model the whole three-dimensional flow.

## Résumé

Dans les écoulements granulaires, les grains les plus gros ont tendance à monter vers la surface, tandis que les grains les plus petits ont tendance à couler vers la base. Cette ségrégation en milieu granulaire est encore mal comprise, particulièrement dans les laves torrentielles, dans lesquelles la combinaison de la ségrégation et du taux de cisaillement important de l'écoulement donne lieu à la formation de bourrelets latéraux canalisant ce dernier.

Nous cherchons à modéliser et à comprendre les propriétés de ces écoulements granulaires. Nous basons notre analyse sur des expériences de grande taille conduites en 2011 [4]. Nous modélisons l'écoulement bidimensionnel du plan centre de l'avalanche, et nous avançons une explication de la structure observée. Nous développons un code modélisant l'écoulement tridimensionnel entier.

# Particle size segregation in granular free-surface flows

## Introduction

The Manchester Centre for Nonlinear Dynamics of the University of Manchester is group of researchers studying nonlinear phenomena. The research notably includes turbulence and bifurcation in fluid dynamics, shock formation and segregation in granular materials. Approximately 25 researchers, with physics or applied mathematics backgrounds are working inside the group.

In nonlinear dynamics, very few theoretical results are available, and the interplay between experiments, theories and simulations is of paramount importance. For example, granular media researchers, though primarily focused on theoretical modelling and computation, are also actively developing three experiments housed in the neighbouring physics building.

During my internship I studied a very specific topic: segregation in granular flows. But since I had no knowledge on granular materials at all when I arrived, I first took interest in understanding what is a granular material, and how we can model and understand it.

The first chapter of the internship report is thus a very general introduction to granular materials and granular flows. At the end of this chapter, we give qualitative ideas about the segregation effect, ideas which are developed more rigorously in the appendix.

The second chapter will focus more specifically on the experiment we seek to model and understand, and on the approach we took to model it.

The third chapter give our results and discuss them.

# Contents

<b>1 General presentation: <i>What is a granular material?</i></b>	<b>4</b>
1.1 Granular materials and granular flows . . . . .	4
1.2 Modelling a granular flow . . . . .	5
1.3 Segregation . . . . .	5
1.3.1 The effect . . . . .	5
1.3.2 The advection equation . . . . .	6
<b>2 The experiment: <i>Segregation effect on a granular free-surface flow down a slope.</i></b>	<b>8</b>
2.1 The experiment . . . . .	8
2.1.1 Setup . . . . .	8
2.1.2 General observations . . . . .	9
2.2 Modelling the experiment . . . . .	9
2.2.1 Constructing the velocity field . . . . .	10
2.2.2 Numerical simulations . . . . .	11
<b>3 Results and discussion: <i>2D and 3D simulations and analytical approach.</i></b>	<b>13</b>
3.1 2D results and discussion. . . . .	13
3.1.1 2D simulations . . . . .	13
3.1.2 Analytical computations . . . . .	14
3.1.3 Applying the change of coordinates to the segregation equation . . . . .	15
3.1.4 Prescribing other velocity fields . . . . .	16
3.2 3D generalisation . . . . .	17
<b>4 Conclusion:</b>	<b>18</b>
<b>A Segregation theory</b>	<b>19</b>
A.1 Physical context . . . . .	19
A.2 Derivation of the segregation equation . . . . .	19
A.2.1 Shallow flows . . . . .	21
A.2.2 Chosing a form for $f^\nu$ . . . . .	21
A.2.3 Additional remarks . . . . .	23
<b>B Finite volume methods</b>	<b>24</b>
B.1 Finite volumes . . . . .	24
B.2 The Lax and Friedrichs scheme . . . . .	25
B.3 The Kurganov and Tadmor scheme . . . . .	25
<b>C Programming</b>	<b>27</b>
C.1 Containers . . . . .	27
C.1.1 Scalar fields . . . . .	27
C.1.2 Flux functions . . . . .	27
C.1.3 Equations . . . . .	28
C.2 Solvers . . . . .	28
C.3 Another approach . . . . .	29

<b>D Method of characteristics</b>	<b>30</b>
D.1 Characteristic curves . . . . .	30
D.2 Change of coordinates . . . . .	31
D.3 Shock waves and jump condition . . . . .	31
D.4 Structure of the solution . . . . .	32

# Chapter 1

## General presentation

*What is a granular material?*

### 1.1 Granular materials and granular flows

In the top of an hourglass, sand is this strange solid. It's at the verge of being a solid, it flows through the middle as something like a liquid, and then it is a solid again.

---

H. M. Jaeger

As exemplified by Jaeger, granular materials such as sand often behave in a liquid-like fashion: they flow, they take the form of their container and they have an horizontal surface. However they are far from being liquids. For example sand falling to the bottom of the hourglass forms a pile, not a flat liquid-like surface. This is because a granular material is highly dissipative. When receiving some energy it tends to disperse it rather than conserve it. This is why it takes a significant amount of energy to make a granular material flow like a liquid. Moreover as this energy is constantly dispersed inside the material, one has to continuously bring energy to the material in order to keep it flowing. At low speeds, grains tend to assemble and cause the flow to stop suddenly. This can be seen as a phase transition called the jamming transition. These two effects, jamming and dispersion, are consequences of the relatively large size of the grains forming a granular material. Smaller grains would be able to reach thermal equilibrium thus behaving like a liquid or a gas.

In fact, a granular material is by definition composed of grains sufficiently large not to be able to reach thermal equilibrium, or to be subject to brownian motion. Grains are by definition interacting only by friction and collision<sup>1</sup>. This is why the smallest grains have a typical radius of 100 micrometers. There is no upper bound for the grains' radius. Ice floes forming the polar ocean's ice cap ranging from a few metres to several kilometres can be seen as the giant grains of a granular material [3].

The most spectacular examples of granular flow are probably debris and pyroclastic flows. Debris flows usually occur in mountains, after a forest fire followed by intense rainfall. The soil is then covered in ashes turning into mud because of the addition of rainwater. The muds begin sliding, carrying with it logs, branches, boulders and even entire trees. All these objects can be seen as grains, though they are of very different shapes and sizes. We will see later that the existence of different sizes of grains in a granular material lead to a spectacular effect called segregation. Pyroclastic flows occur during or shortly after a volcanic explosive eruption. The mixture of rocks and hot gases ejected by the volcano goes down its flanks at high speeds, reaching the base after a few minutes.

It is not surprising that many examples of granular flows are found in industry. After all, sand is the second most used material by human beings after water. Apart from sand, one can observe granular flows in cereal or powder silos, or in various pharmaceutical production lines.

---

1. Smaller particles like powders or colloids are subject to other forces, namely Van der Waals forces or brownian motion forces.

## 1.2 Modelling a granular flow

Because a granular material is a highly dissipative system, it will often not be able to explore all of its accessible phase space. Instead of reaching its equilibrium state, it will dwell into a metastable state. This makes it difficult to describe using the tools of statistical mechanics. For example, doing an ensemble average over all accessible configurations of the system is not possible. Since a granular flow resembles a liquid flow, it will be appropriate to use the tools of fluid mechanics to describe it. This is what we will do in this report.

More precisely, we will make use of the *fluid description* used in fluid mechanics. That is, we make the approximation that the discrete collection of grains can be described by continuous quantities such as pressure, velocity, ... To this aim, we define continuous quantities describing the granular flow as a mean over a volume of grains sufficiently small to be considered infinitesimal, but sufficiently large for the quantities to be independent of local random fluctuations. A volume verifying these properties is called a control volume. For example, the velocity of the granular material at point  $x$  will be defined as the average grains velocity in a small control volume centred at  $x$ .

Most experiments on granular flows are concerned on studying the behaviour of the grains while they go down an inclined plane. Such a flow is typically only 20 or 30 grains high, so it is questionable that a control volume can be defined for such a system. In most cases, however, results from computations using a fluid-like description are in good qualitative and quantitative agreement with experiments [9].

In fluid mechanics, the evolution of the velocity field is driven by the evolution of the pressure and force fields. It is the same for granular materials. Forces exerted on the grains are gravity and friction forces. Friction forces are of two types: the friction exerted on the grains by the bed the granular material is slipping on, and the friction exerted on the grains by their neighbours. The latter is modelled by a viscosity term. Contrary to classical fluids, a granular material will not flow if the base it is lying on is not sufficiently inclined. [10].

This is modelled by a *velocity-dependant* viscosity. This classifies granular flows as non-newtonian fluids. For granular flows, there is no general, universally valid theory. The velocity dependency of the viscosity term is devised experimentally. There is good hope, however, that we can use a reasonably general form for the viscosity. See for example [5].

Another special feature of granular flows is segregation. Most of this report will focus on it. The following section is a general presentation of the segregation effect.

## 1.3 Segregation

### 1.3.1 The effect

Segregation occurs in granular materials composed of grains of different sizes. What we call segregation is the counter-intuitive effect making the largest grains go to the top of the flow, and the small grains sink to the bottom of the flow. It is sometimes called the "Brazil nut effect" because in a mixture of nuts, the Brazil nuts being the largest "grains", then tend to go at the surface. I personally prefer the appellation "muesli effect" since it is at play in our morning mueslis! We always find the largest "muesli particles" such as nuts or banana slices at the surface of our cereal bowl, and the smallest ones at the bottom.

We can explain qualitatively this effect in several ways. A natural way of seeing the segregation effect is to consider that the small particles will fall in the gaps opening between the large ones. Gaps open between large particles when some energy is brought to the system, for example when it is shaken, or when it is mixed with a spoon if it is a muesli mixture, or when it is sheared if it is a granular flow.

But this explanation assumes that large particles are in a sufficient number to form a "matrix" through the holes of which the small grains can fall. In a dilute mixture, when the large grains are no longer in a sufficient number to form a matrix, this point of view is not relevant. In that case, the segregation effect can be explained considering that when some energy is brought to the system, small grains will slip between large ones, and so, by force imbalance, large grains will go upward. Because of the dissipation constantly occurring in granular media, this process is irreversible, and will progressively make large grains go to the surface.

The net result of segregation is the *advection* of small grains downwards, and the advection of large grains upwards. We will model this effect using an advection equation.

### 1.3.2 The advection equation

We are interested in modelling the segregation effect using the fewest possible hypotheses on our physical system. We will discuss in more detail the setup of the system we actually studied during my internship, in the next chapter. For now, let us just assume that we have a granular flow, constituted of a mixture of two different grain types: small and large ones. This assumption is commonly made, since it simplifies greatly the equations, but still captures the essential physical features of segregation. For a more general theory, see [11].

The quantity we are interested in modelling is the proportion of small grains  $\phi^s(\mathbf{r})$  and the proportion of large grains  $\phi^l(\mathbf{r})$  in the neighbourhood of  $\mathbf{r}$ . More precisely, if  $d\tau$  is a small volume of granular material centred at position  $\mathbf{r}$ , and if  $d\tau^s$  is the fraction of this volume occupied by small particles, and  $d\tau^l$  the fraction occupied by large ones, we have

$$\phi^s = \frac{d\tau^s}{d\tau^l + d\tau^s} = \frac{d\tau^s}{d\tau} \quad (1.1)$$

$$\phi^l = \frac{d\tau^l}{d\tau} \quad (1.2)$$

Note that in this description, we implicitly neglect the effects of an interstitial fluid. We can focus on  $\phi^s \equiv \phi$  and completely forget about  $\phi^l$  since  $\phi^l = 1 - \phi$ .  $\phi$  is a non-dimensional number but we will call it *concentration of small particles*. Since the number of particles is a conserved quantity, so is the concentration  $\phi$ . Since the concentration of small particles is conserved in any volume  $\mathcal{V}$  we have

$$\frac{d}{dt} \int_{\mathcal{V}} \phi(\mathbf{r}) d\mathbf{r} = 0 \quad (1.3)$$

We can transform this integral law into a differential law governing the evolution of  $\phi$ . This is a well known procedure, and the reader already familiar with it can skip the next section.

Using the transport theorem,

$$\frac{d}{dt} \int_{\mathcal{V}} \phi(\mathbf{r}) d\mathbf{r} = \int_{\mathcal{V}} \frac{\partial}{\partial t} \phi(\mathbf{r}) d\mathbf{r} + \int_{\partial\mathcal{V}} \phi(\mathbf{r}) \mathbf{v}^s(\mathbf{r}) \cdot d\mathbf{S} \quad (1.4)$$

where  $\partial\mathcal{V}$  is the surface bounding the volume  $\mathcal{V}$ ,  $d\mathbf{S}$  an infinitesimal element of such a surface, and  $\mathbf{v}^s$  the velocity of the small particles. Using Stoke's theorem,

$$\int_{\partial\mathcal{V}} \phi(\mathbf{r}) \mathbf{v}^s(\mathbf{r}) \cdot d\mathbf{S} = \int_{\mathcal{V}} \nabla \cdot (\mathbf{v}^s \phi(r, t)) d\tau \quad (1.5)$$

Since this is true for any volume  $\mathcal{V}$  we have

$$\frac{\partial}{\partial t} \phi + \nabla \cdot (\mathbf{v}^s \phi) = 0 \quad (1.6)$$

Now, what is  $\mathbf{v}^s$ ? We said it was the velocity of the small particles. More precisely, it is the *average* velocity of the small particles enclosed in a small control volume  $d\tau$ . We can also define a velocity  $\mathbf{v}$ , which is defined as the averaged velocity of all particles enclosed on the control volume  $d\tau$ . It is sometimes called the bulk velocity. What is the relation between  $\mathbf{v}$  and  $\mathbf{v}^s$ ? If all particles were small particles, of course we would have

$$\mathbf{v} = \mathbf{v}^s \quad (1.7)$$

and of course no segregation effect will take place. If the segregation effect is not strong, we can treat it as a linear perturbation of the case without segregation:

$$\mathbf{v}^s = \mathbf{v} + \delta\mathbf{v}^s \quad (1.8)$$

We know that segregation occurs only in the vertical direction, ie

$$\delta v_x^s = 0 \quad (1.9)$$

$$\delta v_y^s = 0 \quad (1.10)$$

Moreover, we know that this small term  $\delta \mathbf{v}^s$  must be 0 when all particles are small ones, but also that, symmetrically,  $\delta \mathbf{v}^l = 0$  when all particles are large ones:

$$\delta \mathbf{v}^s(\phi = 1) = 0 \quad (1.11)$$

$$\delta \mathbf{v}^l(\phi = 0) = 0 \quad (1.12)$$

So the simplest form for this term would be

$$\delta \mathbf{v}^s(\phi) = \begin{pmatrix} 0 \\ 0 \\ -q(1-\phi) \end{pmatrix} \quad (1.13)$$

and for large particles:

$$\delta \mathbf{v}^l(\phi) = \begin{pmatrix} 0 \\ 0 \\ q\phi \end{pmatrix} \quad (1.14)$$

where  $q$  is the mean segregation rate, measured experimentally. We will use this expression, from now on<sup>2</sup>.

We can now rewrite the conservation law in terms of  $\mathbf{v}$  and  $\delta \mathbf{v}^s$ :

$$\frac{\partial}{\partial t}\phi + \frac{\partial}{\partial x}u\phi + \frac{\partial}{\partial y}v\phi + \frac{\partial}{\partial z}w\phi - q\frac{\partial}{\partial z}\phi(1-\phi) = 0 \quad (1.15)$$

This is the equation we will use to model the segregation effect. We will call it the *segregation equation*.

---

2. For a more rigorous - but longer! - derivation, see appendix A.

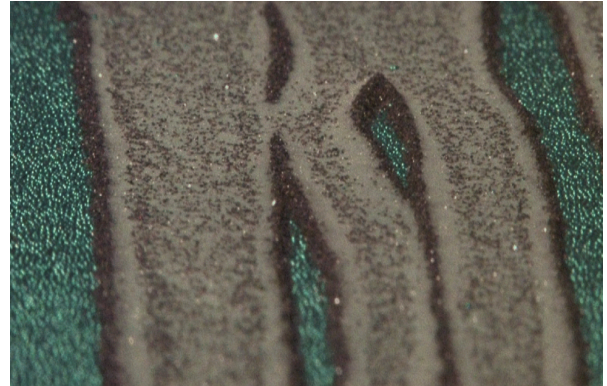
# Chapter 2

## The experiment

*Segregation effect on a granular free-surface flow down a slope.*



(a) 10 metres wide channels formed by pyroclastic flows after Mount St Helen 1980 eruption.



(b) A small scale experiment housed in the University of Manchester, exhibiting channels approx. 2 cm wide.

Figure 2.1: Channelisation is a wide-spread phenomenon.

Segregation effects in granular avalanches are important as they influence overall flow characteristics.

In natural granular flows (fig. 2.1a) and in small scale laboratory experiments (fig. 2.1b) we observe the formation of lateral levees channelising the flow as it goes down a slope.

Though the remains observed in fig. 2.1a provide some information on the characteristics of the flow, it is hard to deduce from these observations the process at play before the material came to rest. Observing natural granular flows as they occur is impractical, due to unpredictability and potential dangers. Though large scale features can be qualitatively reproduced in the laboratory, scaling issues can emerge. It is best to develop large scale experiments to simulate natural debris flow characteristics.

### 2.1 The experiment

#### 2.1.1 Setup

A series of two large scale experiments were conducted in August 2011 at the United States Geological Survey (USGS) debris-flow flume, near Blue River, Oregon [4].

The experimental device consists of a 95 meters long, 2 meters wide inclined channel terminated by a 25 meters long roughly horizontal run-out pad (see fig. 2.2). A mixture of water saturated sand (0.0625-2 mm) and gravel (2-32 mm) is prepared behind the gates closing the channel entrance. When the  $10 m^3$  mixture is released, it accelerates and reaches the end of the channel after  $\approx 10$  seconds. Just after the head of the flow pass the end of the channel, it is truncated and the rest of the flow is diverted

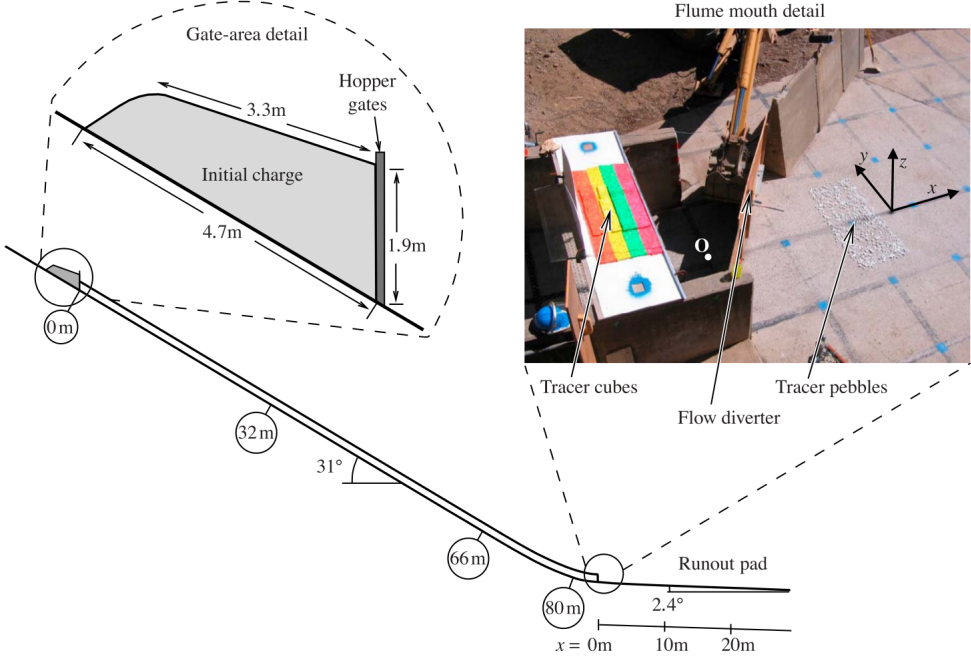


Figure 2.2: Setup of the large-scale experiment.

(see flume mouth detail in fig. 2.2). A measurement of the head's surface velocity is performed by ultra-rapid cameras for the first few meters. During the measurement, the head has an approximately constant velocity of  $u_F = 2.0 \text{ m} \cdot \text{s}^{-1}$ . It then slows down; after a few more seconds the material is deposited on the run-out pad. The rest of the flux is diverted to prevent it from mixing with the head on the run-out pad and bury the initial deposit.

We are interested in studying the last stage of the avalanche, during which the cut head front is going at constant speed on the run-out pad. In the reference frame travelling at the front speed, we observe that the velocity field is stationary. So in that frame, particle paths coincide with streamlines.

### 2.1.2 General observations

The surface of the flow is composed of large gravel particles. This is evidence that segregation effects are at play. Moreover, the formation of lateral levees channelising the flow is observed. How can we qualitatively account for this observation?

A key feature of the experimental flow, also observed in natural debris flow, is the existence of high shear rates, both in the direction of the flow, and in the lateral direction. Sheering in the direction of the flow makes the uppermost layer of particles go faster than the internal layers. When it arrives at the front, it wraps around the head, and the large particles constituting it are buried. Because of segregation effects, they are then pushed up. And because of the existence of a high lateral shear rate, as they go up they will also be pushed to the sides and deposited inside lateral levees.

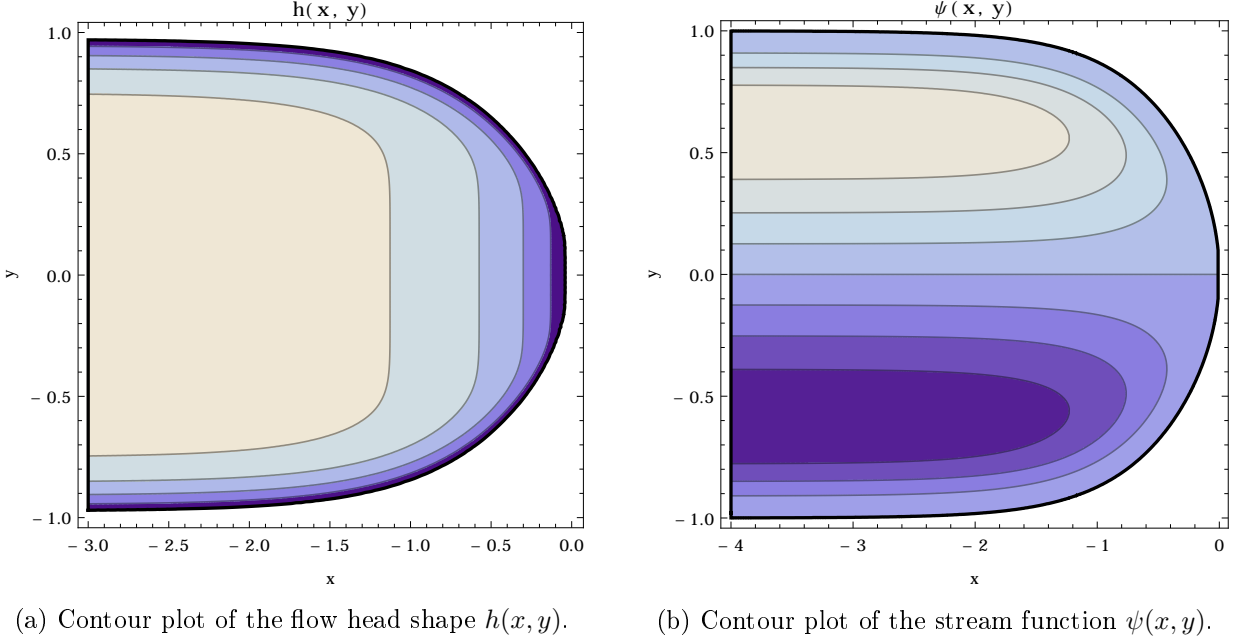
From this qualitative analysis supported by experimental observations, we deduce that it is the interplay between segregation pushing large particles up, and advection pushing large particles down and to the aisles that is responsible for levee formation and channelisation. During this internship, we took interest in modelling and explaining in detail this segregation/recirculation effect.

## 2.2 Modelling the experiment

An option would be to model the experimental flow using fluid equations analogous to the Navier-Stokes equation of fluid mechanics. Prescribing the initial velocity and mass distribution would enable us to deduce the whole evolution of the bulk velocity field. However, it is not trivial to choose a rheology (ie a granular friction law) adapted to the problem, and at the same time not leading to ill-posedness. And since measurement of surface velocity and internal shear stress were performed

during the experiments, it is natural to prescribe a velocity field agreeing with the measurements, and use it to analyse what is going on inside the flow. As we said before, during the phase we analyse, the velocity field is stationary in the travelling frame. Starting from this point, every quantity will be expressed in this reference frame. The axis will be chosen accordingly to what is shown in fig. 2.2: the  $x$  axis is in the direction of the flow, the  $z$  axis is orthogonal to the base, and the  $y$  axis is such that the base is orthonormal and positively oriented.

### 2.2.1 Constructing the velocity field



(a) Contour plot of the flow head shape  $h(x, y)$ .

(b) Contour plot of the stream function  $\psi(x, y)$ .

Figure 2.3

To begin with, we prescribe the shape of the flow surface (fig. 2.3a). There is a general procedure to build a velocity field knowing the flow surface and base, and the *depth-integrated velocity profile*. This quantity is defined as

$$h(x, y)\bar{u}(x, y) = \int_{z=0}^{z=h} u(x, y, z) dz \quad (2.1)$$

Rather than manipulating the velocity components  $u(x, y, z)$ ,  $v(x, y, z)$ ,  $w(x, y, z)$ , we will make use of the *depth integrated velocity components*  $\bar{u}(x, y)$ ,  $\bar{v}(x, y)$ ,  $\bar{w}(x, y)$ . They are defined by

$$h(x, y)\bar{u}_i(x, y) = \int_{z=0}^{z=h} u_i(x, y, z) dz \quad (2.2)$$

Since they only depend on 2 variables instead of 3, they are easier to deal with. In particular, since we assume 3D incompressibility, we have

$$\frac{\partial}{\partial x} h\bar{u} + \frac{\partial}{\partial y} h\bar{v} = 0 \quad (2.3)$$

We can thus define  $\bar{u}$  and  $\bar{v}$  by a single scalar field: the stream function  $\psi(x, y)$ , such that

$$\frac{\partial \psi}{\partial x} = -h\bar{v} \quad (2.4)$$

$$\frac{\partial \psi}{\partial y} = h\bar{u} \quad (2.5)$$

A stream function producing a velocity field in good agreement with the experiments is

$$\psi(x, y) = \frac{HU}{W^2} \left( kyy_0^2 - \frac{k}{2n+1} \frac{y^{2n+1}}{y_0^{2n-2}} - \frac{1}{2m+1} \frac{y^{2m+1}}{y_0^{2m-2}} + \frac{1}{2n+2m+1} \frac{y^{2n+2m+1}}{y_0^{2n+2m-2}} \right) \quad (2.6)$$

where  $H$  is the height of the flow far from the head, and  $W$  and  $U$  respectively the typical width and speed of the flow. They are chosen to fit the experimental data.

We have prescribed the depth-integrated velocity field. To compute the full velocity field, we still need a supplementary information, which is provided by the *velocity profile*, containing the  $z$  dependency of the velocity components It is defined by<sup>1</sup>

$$\begin{pmatrix} u(x, y, z) \\ v(x, y, z) \end{pmatrix} = f\left(\frac{z}{h}\right) \begin{pmatrix} \bar{u}(x, y) \\ \bar{v}(x, y) \end{pmatrix} \quad (2.7)$$

Now we have the full velocity profile. We can use it to deduce the evolution of the concentration in small and large particle using the segregation equation we derived in chapter 1:

$$\frac{\partial}{\partial t} \phi + \frac{\partial}{\partial x} u\phi + \frac{\partial}{\partial y} v\phi + \frac{\partial}{\partial z} w\phi - q \frac{\partial}{\partial z} \phi(1 - \phi) = 0 \quad (2.8)$$

Solving this equation analytically is difficult. So we would like to solve it numerically, to have an idea of its structure.

### 2.2.2 Numerical simulations

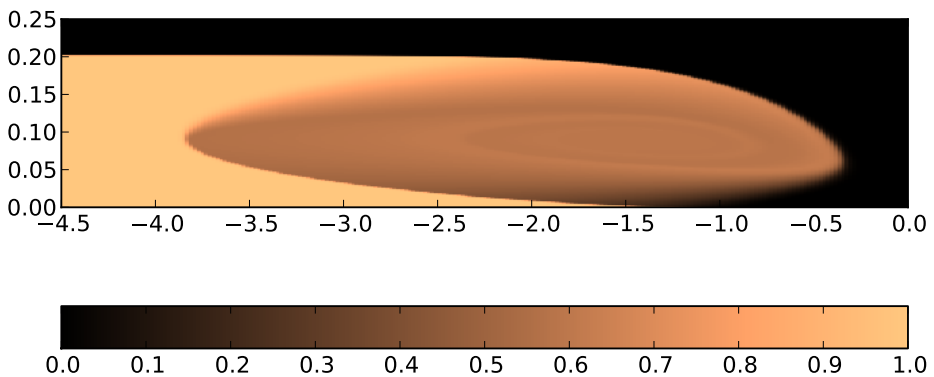


Figure 2.4: Steady-state numerical solution for the 2D problem in the centre plane. Contour plot of the concentration in small particles  $\phi$ . The darkest, the lowest the concentration is. Quantities are adimensional.

Solving conservation laws numerically is a challenging problem. These equations describe quantities that can become discontinuous. For example, a fully segregated granular material is composed of a layer of large particles on top of a layer of small particles. Thus  $\phi = 0$  in the upper part of the system, and  $\phi = 1$  in the lower part. The two domains are separated by a concentration jump.

---

1. Note that this definition of  $f$  implies that  $u$  and  $v$  have the same  $z$  dependency. Though it is not necessarily the case, it has proven a good approximation for the flow we seek to model.

Such jumps are difficult to render numerically, as numerical viscosity tends to smooth out discontinuities.

Various approaches can be used to solve conservation laws numerically. We choose to handle the problem using a *finite volume method*. Details about finite volume methods can be found in appendix B.

Finite volume methods are exact in the sense that they conserve the solved quantity. For us, that means that the *numerically computed* total concentration of small particles in the integration domain coincides with the *exact* total concentration, at any time. This property of conservation is extremely important: it ensures that discontinuities will be accurately calculated by our scheme.<sup>2</sup>

Far from the head the mixture is fully segregated: it is composed of a layer of large particles (20% of the total flow height) on top of a layer of small particles (80% of the total height). They are separated by a sharp discontinuity in the concentration  $\phi$ , called a *shock wave*. Close to the head, because of the shearing process, the layer of large particles wraps around the layer of smalls. This gives rise to a complex structure, which we would like to explore numerically. We set the initial particles to occupy the 0.8 lowest fraction of the flow height. We then let the system evolve until it reach a steady state. Before we simulate the whole 3D flow, we will start with a 2D simulation in the centre plane, ie the plan  $y = 0$ . Indeed in this plane,  $\partial v / \partial y = 0$ , which means that particles in the centre plane stay in the centre plane. We can rewrite the segregation equation:

$$\frac{\partial}{\partial t} \phi + \frac{\partial}{\partial x} u\phi + \frac{\partial}{\partial z} w\phi - q \frac{\partial}{\partial z} \phi(1 - \phi) = -v \frac{\partial}{\partial y} \phi \quad (2.9)$$

The term  $-v \partial \phi / \partial y$  can be seen as a source term in the 2D problem. For a brief explanation of how the code I developed during the internship works, see appendix C. The resulting steady-state solution is shown in fig 2.4.

The structure of this solution is higly interesting, and will be analysed in the next chapter.

---

2. It can be easily shown (Lax-Wendroff theorem [7]) that finite-volume schemes, provided that they converge, will converge to a -perhaps discontinuous- solution of the *exact* conservation law, while non conservative schemes whilst doing as well as finite-volume methods every time the solution is continuous, will cease to be accurate if the solution has discontinuities. Since discontinuities are an essential feature of conservation laws, the conservative property of finite-volume methods is of the highest importance.

# Chapter 3

## Results and discussion

*2D and 3D simulations and analytical approach.*

### 3.1 2D results and discussion.

#### 3.1.1 2D simulations

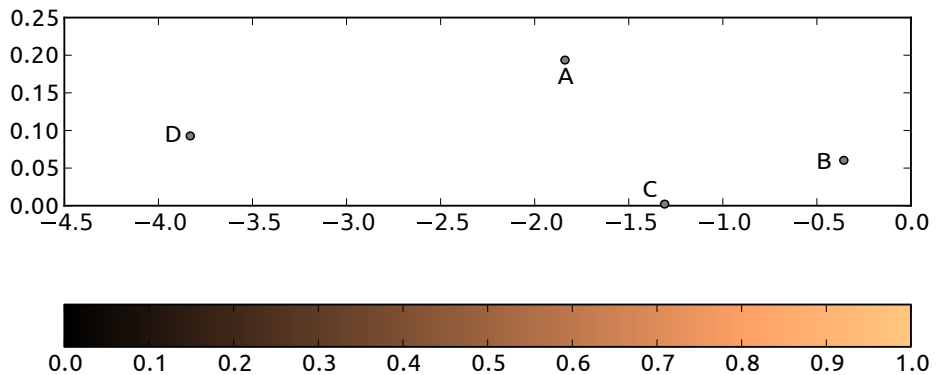


Figure 3.1: Steady state numerical solution for the 2D in the centre plane.

The structure of the steady state can be very well explained qualitatively. Far from the head of the flow, the mixture is fully segregated. This is understandable: enough energy was given by the shearing process for the mixture to segregate during the flow's way down to the run-out pad.

Closer from the head, a complex lens-shaped structure appears. It is delimited by two jumps in the concentration<sup>1</sup>, one from  $A$  to  $B$ , the other from  $C$  to  $D$  (cf fig. 3.1). From  $B$  to  $C$  and from  $D$  to  $A$  the interface is dilute. It is what is called a rarefaction fan. Such fans are a common feature of

1. See annex B for more details on jumps in segregation equations

conservation laws.

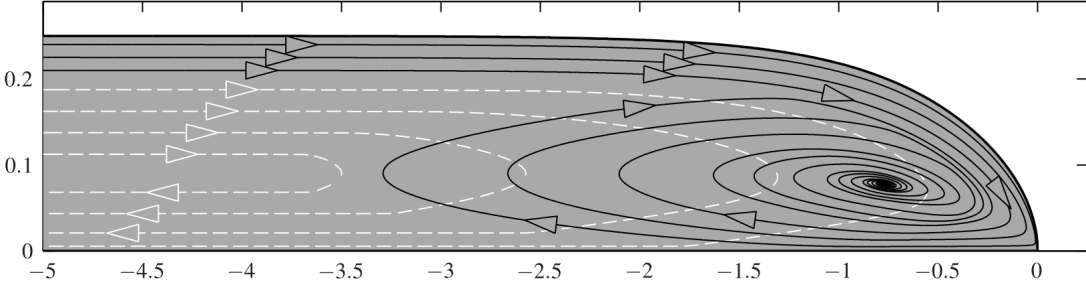


Figure 3.2: Large particles paths (black lines) and small particles paths (white dotted lines) in the centre plane.

Inside the lens, we observe a mixture of small and large particles. If we compute the large particles trajectories (cf fig. 3.2), we understand more clearly what is going on: large particles are going to the head faster than small ones. Therefore they are buried to the base of the flow, where they experience segregation. The combination of these two antagonist effects result in a spiral-like structure.

It is important to note, that if  $\partial v / \partial y$  is zero, this spiral-like structure will *not* appear. Cf for exemple [2]. In this article, a setup very similar to ours, but truly two dimensional is studied analytically. A similar lens-like structure is found to exist close to the head, and for the same reason. But here, because of the truly 2D nature of the problem, no spiral is observed.

The existence of a  $\partial v / \partial y$  term implies that the 2D flow we analyse in the centre plane is compressible:

$$\frac{\partial u}{\partial x} + \frac{\partial w}{\partial z} = -\frac{\partial v}{\partial y} \neq 0 \quad (3.1)$$

Qualitatively, this shows that some material from regions close to the centre plane is lost as it is advected to the sides of the flow. This advection occurs only close to the head, where the  $\partial v / \partial y$  term is the highest in modulus.

### 3.1.2 Analytical computations

The geometrical *method of characteristics* enables us to solve segregation equations in some particular situations. See appendix D to see how it is done with a very simple example. Following what we did in appendix D for the simplified segregation equation, we can do a change of coordinates to study the structure of our solution. There is, however, a major difference between the two dimensional flow we studied in appendix D and the one we study now. In the simplified 2D case, the idea was to remap the  $z$  axis:

$$z \leftarrow \psi(x, z) \quad (3.2)$$

where  $\psi$  is the stream function defined by

$$\begin{pmatrix} \frac{\partial \psi}{\partial x} \\ \frac{\partial \psi}{\partial z} \end{pmatrix} = \begin{pmatrix} -w \\ u \end{pmatrix} \quad (3.3)$$

Using the symmetry of second derivatives we see that the definition of  $\psi$  implies

$$\frac{\partial u}{\partial x} + \frac{\partial w}{\partial z} = 0 \quad (3.4)$$

which is the incompressibility condition for a 2D flow. Of course in 3D the incompressibility condition is

$$\frac{\partial u}{\partial x} + \frac{\partial v}{\partial y} + \frac{\partial w}{\partial z} = 0 \quad (3.5)$$

so we cannot define a stream function. We need to use another function to remap the  $z$  axis.

We notice that for a 2D stationary flow, the lines  $\psi(x, z) = 0$  are the particle paths<sup>2</sup>. So in the 3D case, rather than remapping the  $z$  axis with a stream function, which is impossible, we will just say that our new  $z$  coordinate is a -for now- unknown function  $\zeta(x, z)$  which is constant along particle paths.

This property implies that

$$\begin{pmatrix} \frac{\partial \zeta}{\partial x} \\ \frac{\partial \zeta}{\partial z} \end{pmatrix} \propto \begin{pmatrix} -w \\ u \end{pmatrix} \quad (3.6)$$

Let us call  $\lambda(x, z)$  the coefficient of proportionality. Of course if  $\lambda(x, z) = 1$  we have again

$$\frac{\partial u}{\partial x} + \frac{\partial w}{\partial z} = 0 \quad (3.7)$$

so let us assume to begin with that  $\lambda$  is a function of  $\zeta$  only :  $\lambda(x, z) = \hat{\lambda}(\zeta)$

Expressing the velocity components in terms of derivatives of  $\zeta$  in the 3D incompressibility equation yields

$$-\underbrace{\left( u \frac{\partial}{\partial x} + w \frac{\partial}{\partial z} \right)}_{\equiv D^\perp} \log \lambda(x, z) + \frac{\partial v}{\partial y} = 0 \quad (3.8)$$

The operator  $D^\perp$  appearing in the formula above plays a particular role. Indeed if we call  $\zeta^\perp$  a coordinate locally orthogonal to  $\zeta$  we can easily see that

$$D^\perp = u \frac{\partial}{\partial x} + w \frac{\partial}{\partial z} \propto \frac{\partial}{\partial \zeta^\perp} \quad (3.9)$$

so, if  $\lambda(x, z) = \hat{\lambda}(\zeta)$  we have  $D^\perp \hat{\lambda}(\zeta) = 0$  and thus again

$$\frac{\partial u}{\partial x} + \frac{\partial w}{\partial z} = 0 \quad (3.10)$$

Since making  $\lambda$  dependant or not on  $\zeta$  does not have any impact on eq. (3.8) I am going to assume for now on that  $\lambda$  is not a function of  $\zeta$ . In the system of coordinates  $(x, \zeta)$  we can define  $\lambda$  as a function of  $x$  only :  $\lambda = \lambda(x)$ . In this system of coordinates,  $D^\perp = u \frac{\partial}{\partial x}$  and thus

$$-u \frac{d}{dx} \log \lambda + \frac{\partial v}{\partial y} = 0 \quad (3.11)$$

Integrating this first order ordinary differential equation will give us  $\lambda(x)$  up to an arbitrary integration constant. Knowing  $\lambda(x)$ , we can in turn know  $\zeta(x, z)$ , again up to an integration constant, using

$$\begin{pmatrix} \frac{\partial \zeta}{\partial x} \\ \frac{\partial \zeta}{\partial z} \end{pmatrix} = \lambda(x) \begin{pmatrix} -w \\ u \end{pmatrix} \quad (3.12)$$

If we do that, we will have completely defined our change of coordinate  $z \leftarrow \zeta$  and we will know it explicitly. But is it useful to do this change of coordinates? Does it make it easier to find the structure of the steady-state solution as in the 2D case? We will see that it is indeed the case in the next section.

### 3.1.3 Applying the change of coordinates to the segregation equation

After the change of coordinates, the segregation equation becomes

$$\frac{\partial \phi}{\partial x} - \lambda(x) \frac{\partial}{\partial \zeta} \phi (1 - \phi) = 0 \quad (3.13)$$

This equation is exactly the one we have in the 2D case from appendix D, after doing the change of coordinate  $z \leftarrow \zeta(x, z) = \psi(x, z)$ , except that in that case  $\lambda(x) = 1$ .

---

2. Note that for a granular polydisperse flow, what we call "particle paths" are not the paths followed by actual particles. It is rather the paths of hypothetical particles having their velocity equal to the bulk velocity.

Let  $\zeta = Z(x)$  be a characteristic curve. And let us call  $\Phi$  the (constant) value of  $\phi(x, \zeta)$  along the characteristic curve. We have

$$\frac{dZ}{dx} = -\lambda(x)(1 - 2\Phi) \quad (3.14)$$

Because  $\lambda$  depends on  $x$  characteristics are not straight lines, contrary to what happens in the 2D case. To get around this problem, we can remap the  $x$  axis :  $x \leftarrow \xi(x)$ . In this new system of coordinates, characteristics will be straight lines if and only if

$$\frac{d\xi}{dx} = \lambda(x) \quad (3.15)$$

and the segregation equation becomes

$$\frac{\partial\phi}{\partial\xi} - \frac{\partial}{\partial\zeta}\phi(1 - \phi) = 0 \quad (3.16)$$

In this new coordinates system the jump condition<sup>3</sup> is of course simply the same as in the simplified case:

$$\frac{d\zeta}{d\xi} = \phi^+ + \phi^- - 1 \quad (3.17)$$

The equation is the same as in 2D case, but we expect the solution to be different. Namely, to exhibit a "spiral" structure. Why is this spiral appearing? An hypothesis is that since the horizontal and vertical coordinates  $\xi$  and  $\zeta$  can *both* take the same value for different values of  $x$  and  $z$ <sup>4</sup>, the spatial domain in the remapped coordinates is a mosaic of smaller domains inside which  $\xi$  and  $\zeta$  do not take the same value for different values of  $x$  and  $z$ , each small domain forming a part of the spiral.

Sadly, trying to apply the method to the actual velocity field prescribed in the paper did not work. Indeed, the velocity components have a rather complex analytical expression:

$$u(x, z) = \left( \alpha - \frac{2(\alpha - 1)z}{H\sqrt{-\tanh(\frac{x}{W})}} \right) \left( \frac{(2n + 1)U\sqrt{-\tanh(\frac{x}{W})}}{(2m + 1)(2m + 2n + 1)} + u_F \right) - u_F \quad (3.18)$$

$$w(x, z) = \frac{-z}{2HW} \operatorname{csch}\left(\frac{x}{W}\right) \operatorname{sech}\left(\frac{x}{W}\right) \left( \frac{(2n + 1)U(2(\alpha - 1)z - \alpha H\sqrt{-\tanh(\frac{x}{W})})}{(2m + 1)(2m + 2n + 1)} + \frac{(\alpha - 1)u_F z}{\sqrt{-\tanh(\frac{x}{W})}} \right) \quad (3.19)$$

### 3.1.4 Prescribing other velocity fields

We were able to reproduce this spiral structures with a variety of different velocity fields. This is not surprising, if we have in mind that the origin of the spiral is 2D compressibility. There is therefore hope that we will eventually find a simpler velocity field, but for now, the simplest one we have been able to derive which still exhibit a spiral structure (fig 3.3) is still too complex:

$$u = \left( \alpha + \frac{2(\alpha - 1)z(W - x)}{Hx} \right) \left( u_F - \frac{(2n + 1)Ux}{(2m + 1)(2m + 2n + 1)(W - x)} \right) - u_F$$

$$w = \frac{z \left( \frac{(2n + 1)U(x(\alpha H - 2(\alpha - 1)z) + 2(\alpha - 1)Wz)}{(2m + 1)(2m + 2n + 1)} - \frac{(\alpha - 1)u_F z(W - x)^2}{x} \right)}{H^2}$$

---

3. cf Appendix B

4. in other words the inverse mapping  $x = x(\xi, \zeta)$  and  $z = z(\xi, \zeta)$  is multivalued

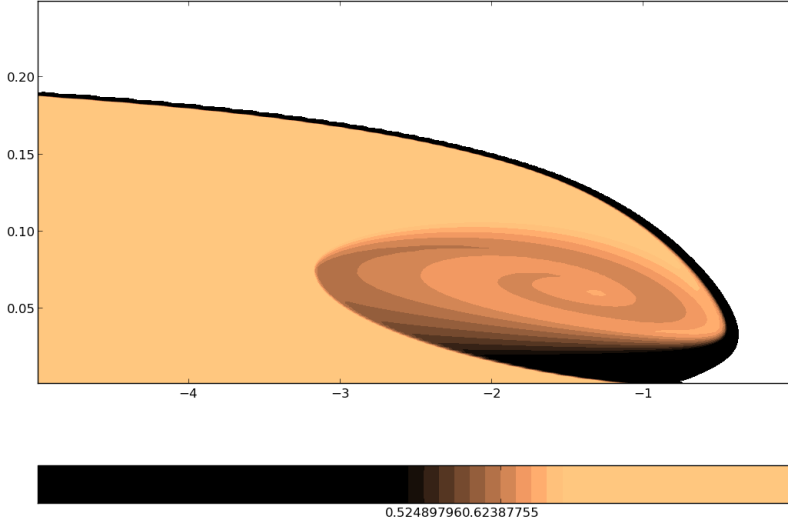


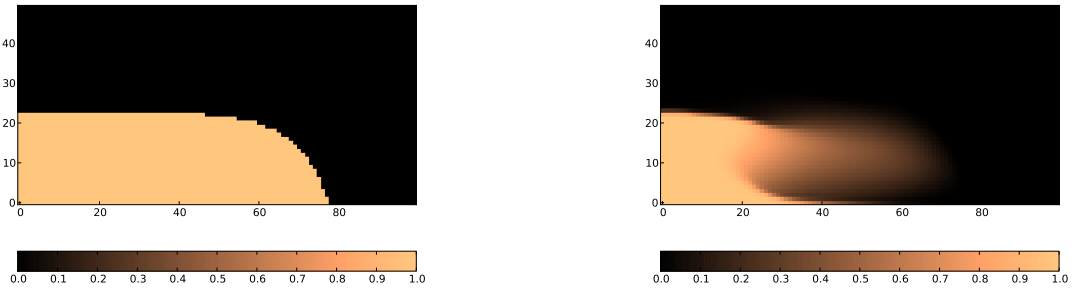
Figure 3.3: Steady-state numerical solution for the simplified velocity profile. The spiral structure is preserved.

### 3.2 3D generalisation

The main goal of the internship was to produce a code capable of solving the full 3D problem as well as the 2D centre plane problem. We chose to implement the Kurganov and Tadmor (KT) scheme [6]. One of the advantages of this numerical scheme is that it is intrinsically dimension-independent. This allowed us to develop a code that can solve partial differential equations in any number of spatial dimensions.

We first ran the code with the 2D problem in the centre plane, to make sure the results were in perfect agreement with the older code used in [4].

Then, we ran it for the full 3D setup. The result is of course impossible to plot, but we can visualize the restriction of the three dimensional concentration to a plan  $y = \text{cst}$ . The results produced by these 3D simulations will be analysed in the future.



(a) Initial concentration close to the aisles of the flow. (b) Concentration at the same location after some time.

Figure 3.4: The structure of the 3D flow is yet to be analysed.

# Chapter 4

## Conclusion

During this internship, I discovered a domain of physics I new nothing about before. We are only beginning to understand the strange physics of granular materials, and it was exciting to be part of this adventure for a few weeks. I feel like I only scratched the surface of the subject, and yet I learned an enormous amount of physics, mathematical techniques and programming during my internship. I learned about how to describe and model granular flows. I learned about the mathematical difficulties arising from these models<sup>1</sup>. I also learned about the strange phenomenon of segregation, and how to model it. It is then that I read about the mathematical theory of hyperbolic partial differential equations, and how to solve this type of equations numerically.

The main goal of my internship was to develop a code to solve the 3D segregation equation. At the end, the code could be used to solve systems of hyperbolic equations

$$\begin{aligned} \frac{\partial}{\partial t} u_1 + \sum_{i=1}^n \frac{\partial}{\partial x_i} f_{1i}(\mathbf{u}, \mathbf{x}) &= 0 \\ &\vdots \\ \frac{\partial}{\partial t} u_m + \sum_{i=1}^n \frac{\partial}{\partial x_i} f_{mi}(\mathbf{u}, \mathbf{x}) &= 0 \end{aligned} \tag{4.1}$$

where  $\mathbf{u}(t, \mathbf{x})$  is the unknown  $m$ -dimensional field living in a  $n$ -dimensional space (in our case, it is the scalar field  $\phi$  living in a 3D space). Since it is very general, one can use this code to solve a lot of different physical problems, and it will be re-used later on.

During the last two weeks of my internship, I took interest in the theoretical side of the problem: namely, how to explain analytically the spiralling structure observed in the simulations and the experiments. Although I did not succeed in doing it, it was really interesting to learn how to solve hyperbolic equations. In particular, I was fascinated by the elegance of the change of coordinates used to solve 2D segregation equations, as detailed in appendix D.

It was my job as an intern to do simulations and analytical computations. But I also had the great opportunity to toy with some of the small-scale granular experiments hosted in the University of Manchester. This internship made me understand the fundamental importance of the interplay between experiments, simulations and analytical computations.

---

1. namely ill-posedness. I chose not to talk about it in this report, as it is not required to understand the segregation equation, which is the central equation studied during my internship.

# Appendix A

## Segregation theory

### A.1 Physical context

In this appendix, I will give a simple derivation of the equation we used to model the segregation process taking place in granular flows.

We consider a granular flow going down a slope. For the sake of simplicity, we will assume that the granular material is a mixture of small and large particles. This assumption is commonly made, since it simplifies greatly the equations, but still captures the essential physical features of segregation. Through this section  $s$  and  $l$  superscripts will respectively refer to small and large particles. For example the mass of a small particle will be labelled  $m^s$ . As usual, we model the granular flow using the tools of continuum mechanics.

The idea is to see the set of large particles in the material as a matrix through the holes of which small particles can fall. If the material is a still, initially homogeneous mixture of small and large particles, it will partially segregate (leaving the uppermost layers full of large particles, the lowermost full of small particles.). In this case middle layers are a mixture of small and large particles. If the material is a flowing, initially homogeneous mixture of small and large particles, it will completely segregate. This is because as the material flows down the slope, the local void ratio of the large particles matrix fluctuate, causing small to fall into newly opening gaps. The result is a progressive migration of small particles to the bottom. Because of force imbalance, large particles are pushed upward as small particles go downward. After some time, the material will be constituted of a layer of large particles topping a layer of small particles.

### A.2 Derivation of the segregation equation

Let us start by writing down the momentum and force balances for each one of the 2 constituents

$$\partial_t \rho^\nu u_i^\nu + \partial_j \rho^\nu u_i^\nu u_j^\nu = -\partial_i p^\nu + \rho^\nu g_i + \beta_i^\nu \quad (\text{A.1})$$

where

- $\rho^\nu$  is the density of the constituent  $\nu$  ( $\nu = s, l$ ), ie the mass of constituent  $\nu$  per unit volume:

$$\rho^\nu = n^\nu m^\nu$$

where  $m^\nu$  is the mass of a particle of the constituent  $\nu$  and  $n^\nu$  the number of particles of the constituent  $\nu$  per unit volume Note that if  $d\tau$  is a small volume,  $d\tau^\nu$  the fraction of this small volume occupied by the constituent  $\nu$ , and  $\rho^{*\nu}$  the intrinsic density of constituent  $\nu$ ,

$$\rho^\nu = \frac{d\tau^\nu}{d\tau} \rho^{*\nu} = \phi^\nu \rho^{*\nu} \quad (\text{A.2})$$

$\phi^\nu$  is called the *volume fraction* of constituent  $\nu$ . This expression for  $\rho^\nu$  will be useful later.

$$\rho^s + \rho^l = \frac{d\tau^s + d\tau^l}{d\tau} = \rho$$

- $u^\nu$  is the velocity of constituent  $\nu$  averaged on the volume  $d\tau$
- $p^\nu$  is the partial pressure of the constituent  $\nu$ . For convenience we will define  $f^\nu$  as

$$p^\nu = f^\nu p \quad (\text{A.3})$$

–  $\beta^\nu$  is the force exerted by the other constituent on the constituent  $\nu$ .

We assume that each constituent has the same intrinsic density:  $\rho^{*s} = \rho^{*l} = \rho$ . This is usually a good approximation for granular materials.

We can consider the set of large particles as a matrix inside the holes of which small particles are percolating (flowing downwards). It is as if small particles were flowing through a porous medium. In that case, we know that the force exerted by the medium on the particles is

$$\beta^s = p \partial_i f^s - \rho^s c (u_i^s - u_i) \quad (\text{A.4})$$

this form for  $\beta$  is known as Darcy's law, and is frequently used, for example to model the percolation of water through sand.

Symmetrically, we can consider the set of small particles as a matrix inside which large particles are percolation (upwards, this time), and we have

$$\beta^l = p \partial_i f^l - \rho^l c (u_i^l - u_i) \quad (\text{A.5})$$

Segregation is a gravity-induced effect. It will happen in the vertical direction. This means that if  $w$  is the velocity component along vertical axis,

$$u^\nu = u \quad (\text{A.6})$$

$$v^\nu = v \quad (\text{A.7})$$

$$w^\nu \neq w \quad (\text{A.8})$$

It also follows from this assumption that

$$\beta_x^\nu = 0 \quad (\text{A.9})$$

$$\beta_y^\nu = 0 \quad (\text{A.10})$$

$$\beta_z^\nu \neq 0 \quad (\text{A.11})$$

In our case  $w$  is not quite along vertical axis, because of the small angle  $\theta$  the base of the inclined plan makes with the horizontal direction. However, A.6 and A.9 are still valid at first order in  $\theta$ , so we will assume they still hold.

Thus, we will focus on the projection along  $Oz$  of A.1:

$$\partial_t \rho^\nu w^\nu + \partial_j \rho^\nu w^\nu u_j^\nu = -\partial_z (p f^\nu) - \rho^\nu g \cos \theta + \beta_z^\nu \quad (\text{A.12})$$

which, making use of Darcy's law for  $\beta$  we can rewrite as

$$\partial_t \rho^\nu w^\nu + \partial_j \rho^\nu w^\nu u_j^\nu = -f^\nu \partial_z p - \rho^\nu g \cos \theta - \rho c (w^\nu - w) \quad (\text{A.13})$$

In shallow waters, vertical pressure gradient  $\partial_z p$  is approximately hydrostatic. This follows from the fact that acceleration in the  $Oz$  direction is very small compared to vertical pressure gradient. This assumption allows us to simplify our previous equation:

$$0 = -f^\nu \rho g \cos \theta - \rho^\nu g \cos \theta - \rho c (w^\nu - w) \quad (\text{A.14})$$

Now let us see why, in shallow waters, this assumption is true. If you do not want to read the proof, you can jump directly to the next subsection.

### A.2.1 Shallow flows

For the sake of simplicity we will assume that acceleration in  $Oy$  direction is zero:  $\partial_y v = 0$ .

Let  $\Delta x$  and  $\Delta z$  be the typical vertical and horizontal extent of the flow. Assuming that the flow is shallow is equivalent to saying that

$$\Delta z \ll \Delta x \quad (\text{A.15})$$

This and incompressibility, are the two key assumptions we will need to prove our statement. Let  $U$  and  $W$  be the typical value of  $u$  and  $w$ . We have

$$\frac{U}{\Delta x} = \mathcal{O}\left(\frac{\partial u}{\partial x}\right) \quad (\text{A.16})$$

$$\frac{W}{\Delta z} = \mathcal{O}\left(\frac{\partial w}{\partial z}\right) \quad (\text{A.17})$$

Using incompressibility, we have

$$\frac{\partial u}{\partial x} = \mathcal{O}\left(\frac{\partial w}{\partial z}\right) \quad (\text{A.18})$$

ie

$$\frac{U}{\Delta x} = \frac{W}{\Delta z} \quad (\text{A.19})$$

Using momentum and forces balances *for the mixture of the two components*, in projection along  $Ox$  gives

$$\rho(u\partial_x u + w\partial_z u) = -\partial_x p + g \sin \theta \quad (\text{A.20})$$

$g \sin \theta$  is very small compared to pressure gradient, since  $\theta$  is close to 0. Thus we have

$$\mathcal{O}(\rho(u\partial_x u + w\partial_z u)) = \mathcal{O}(-\partial_x p) \quad (\text{A.21})$$

ie

$$\frac{\rho U^2}{\Delta x} = \frac{p}{\Delta x} \quad (\text{A.22})$$

Now using momentum and forces balance for the mixture, in projection along  $Oz$  we have

$$\rho(u\partial_x w + w\partial_z w) = -\partial_z p - g \cos \theta \quad (\text{A.23})$$

What we want to prove is that the acceleration, ie the left hand side of the above equation is very small compared to the vertical pressure gradient, ie the  $\partial_z p$  term. Using successively A.22 and A.19 it is fairly easy:

$$\frac{\mathcal{O}(\rho(u\partial_x w + w\partial_z w))}{\mathcal{O}(\partial_z p)} = \frac{\rho W^2 / \Delta z}{p / \Delta z} = \frac{W^2}{U^2} = \frac{\Delta z^2}{\Delta x^2} \ll 1 \quad (\text{A.24})$$

Thus A.23 is approximately

$$\partial_z p = -g \cos \theta \quad (\text{A.25})$$

The pressure gradient is approximately hydrostatic, as announced, and the simplification leading us to A.12 is justified.

### A.2.2 Chosing a form for $f^\nu$

Using A.2, A.12 can be rewritten as

$$\phi^\nu w^\nu = \phi^\nu w + (f^\nu - \phi^\nu) \frac{g}{c} \cos \theta \quad (\text{A.26})$$

We have  $w^\nu$  as a function of  $w$ . We are almost done! We only need to specify the form of  $f^\nu$ . Before trying something, let us recapitulate what we know about  $f^\nu$ . Recall that

$$p^\nu = f^\nu p \quad (\text{A.27})$$

Since  $p^s + p^l = p$ , we have

$$f^s + f^l = 1 \quad (\text{A.28})$$

Moreover, we know that if the material is composed only of small particles, or of large ones, there is now segregation. In those cases  $w^\nu = w$ . Thus we know that

$$f^\nu(\phi^s = 0, 1) = \phi^\nu \quad (\text{A.29})$$

Let us sum up what we know about  $f^\nu$  graphically:

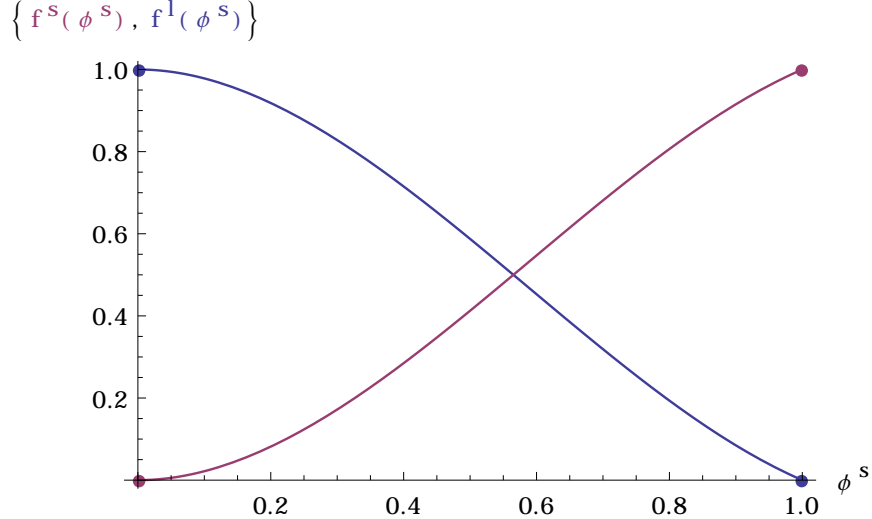


Figure A.1: A possible form for  $f^s$  and  $f^l$ .

Of course the curves for  $f^s$  and  $f^l$  can be different. We only require that  $f^s + f^l = 1$  and that  $f^\nu(\phi^s = 0, 1) = \phi^\nu$ .

The simplest form for the curves would be straight lines:

$$f^\nu = \phi^\nu \quad (\text{A.30})$$

But in that case using A.26 we see that

$$w^\nu = w \quad (\text{A.31})$$

So if the curves  $f^\nu(\phi^s)$  are straight lines, there is no segregation!

We can imagine expanding  $f^s$  and  $f^l$  in powers of  $\phi^s, \phi^l$ .

$$f^\nu = \underbrace{\phi^\nu}_{\text{order 1}} + \underbrace{A_1^\nu \phi^s \phi^l}_{\text{order 2}} + \underbrace{A_{21}^\nu \phi^s (\phi^l)^2 + A_{22}^\nu (\phi^s)^2 \phi^l}_{\text{order 3}} + \dots \quad (\text{A.32})$$

We know that at order 1, there is no segregation effect. So we will expand  $f$  up to order 2 in order to model segregation:

$$f^\nu = \phi^\nu + A_1^\nu \phi^s \phi^l \quad (\text{A.33})$$

since  $f^s + f^l = 1$  we have

$$A_1^s + A_1^l = 0 \quad (\text{A.34})$$

Let  $B = -A_1^s$ . We have

$$f^s(\phi^s) = \phi^s - B\phi^s(1 - \phi^s) \quad (\text{A.35})$$

$$f^l(\phi^s) = 1 - \phi^s + B\phi^s(1 - \phi^s) \quad (\text{A.36})$$

Using again A.26 we obtain the vertical velocities for the small and large particles. They are respectively

$$w^s = w - \frac{Bg \cos \theta}{c}(1 - \phi^s) \quad (\text{A.37})$$

$$w^l = w + \frac{Bg \cos \theta}{c}\phi^s \quad (\text{A.38})$$

Note that  $q = Bg \cos \theta / c$  is the mean segregation velocity. The coefficients  $B$  and  $c$  are unknown, but  $q$  can be measured directly experimentally.

Substituting  $w^s$  the mass balance equation for small particles, we obtain the so-called *segregation equation* for small particles:

$$\partial_t \phi^s + \partial_x u \phi^s + \partial_y v \phi^s + \partial_z w \phi^s - \partial_z q \phi^s (1 - \phi^s) = 0 \quad (\text{A.39})$$

Of course, we have a similar equation for large particles:

$$\partial_t \phi^l + \partial_x u \phi^l + \partial_y v \phi^l + \partial_z w \phi^l + \partial_z q \phi^l (1 - \phi^l) = 0 \quad (\text{A.40})$$

### A.2.3 Additional remarks

Note that doing the transformation  $B \leftarrow -B$  is equivalent to doing  $g \leftarrow -g$ , ie inverting the gravity. Moreover doing the transformation  $\phi^s \leftarrow \phi^l$  is equivalent to exchanging the role of small and large particles. Also notice that

$$f^\nu(\phi^l = 1 - \phi^s; -B) = f^\nu(\phi^s; B) \quad (\text{A.41})$$

That means that the "dual" physical system in which the role of large and small particles is exchanged and the gravity inverted behaves exactly as the normal one. Another way to put it is to say that a large particle in a medium of small ones will be subject to the same force as a small particle in a medium of large ones. Only the direction of the force will be changed. It is not clear at all that this symmetry between a system and its dual exists in real life granular media.

In fact, this symmetry is a special feature on the expansion at order 2 of A.32. At order 3, it disappears. Experiments and finite elements simulations have shown that there is a slight violation of the symmetry between a system and its dual. A third order theoretical model is currently developed to account for this effect and test its implications.

# Appendix B

## Finite volume methods

The aim of this appendix is to explain qualitatively the numerical methods we used during this internship. Readers looking for a more rigorous - but longer! - presentation of such methods can read [8].

For the sake of simplicity, we will focus on the one-dimensional conservation law:

$$\frac{\partial}{\partial t} u(t, x) + \frac{\partial}{\partial x} f(u(t, x)) = 0 \quad (\text{B.1})$$

where  $f$  is called the flux function, and where  $u(t, x)$  is the unknown solution of the equation we seek to approach numerically. Of course, for us this unknown function is the concentration  $\phi$ , but it can be another quantity in the general case. Historically, finite volume methods were developed to solve problem from gas dynamics, hence the use of the conventional letter  $u$  to label the solution, which in this context is the gas velocity.

### B.1 Finite volumes

The idea of finite volume methods is to discretise the physical -here one-dimensional- space into small volume elements called cells. Each cell hold two bits of information: the approximate value of the solution inside the cell, and the approximate value of the flux at each edge of the cell. Cells are usually rectangular, but it is of course not a requirement. We will also discretise time in small intervals  $\Delta T$  called time steps.

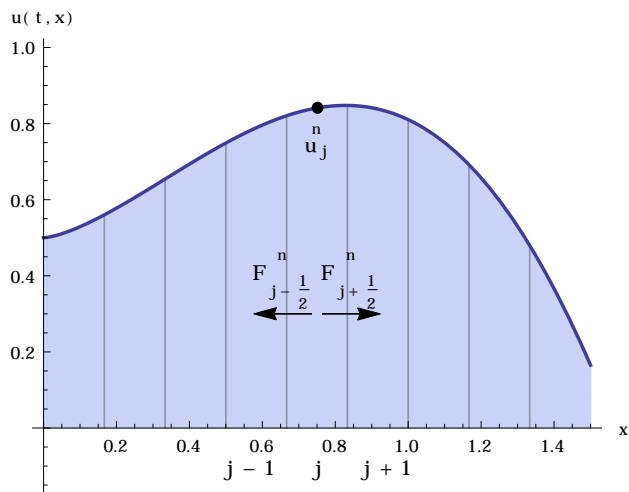


Figure B.1:  $x \rightarrow u(t, x)$  and its discretisation.

We will call  $u_j^n$  the approximate value of the  $u$  function at cell number  $j$  after  $n$  time steps. We will call the fluxes at the right and left edges of this cell  $F_{j+1/2}^n$  and  $F_{j-1/2}^n$ <sup>1</sup>.

---

1. Note that by convention the subscript  $j + 1/2$  ( $j - 1/2$ ) denote the value of a quantity at the right (left)  $j^{\text{th}}$  cell

What we want to do is combine these different quantities to create a numerical scheme. The simplest scheme one can think of is obtained replacing derivatives in the conservation by finite differences:

$$\frac{u_j^{n+1} - u_j^n}{\Delta T} + \frac{f(u_{j+1}^n) - f(u_j^n)}{\Delta x} = 0 \quad (\text{B.2})$$

This scheme involves the cell at position  $j$ , its right neighbour at  $j+1$ , but not its left neighbour at  $j-1$ . This asymmetry between left and right can be an advantage in particular situations, for example if we know that  $u$  is advected from left to right. To get rid of this asymmetry and produce a more generally adapted scheme, we can use central differencing:

$$\frac{u_j^{n+1} - u_j^n}{\Delta T} + \frac{f(u_{j+1}^n) - f(u_{j-1}^n)}{2\Delta x} = 0 \quad (\text{B.3})$$

However one can show that this scheme is unstable. The simplest generally adapted and stable scheme has been proposed for the first time by Lax and Friedrichs in [1].

## B.2 The Lax and Friedrichs scheme

To get the Lax and Friedrichs scheme from the above equation, we simply replace  $u_j^n$  by the mean value over the left and right cells:

$$\frac{u_j^{n+1} - \frac{u_{j+1}^n + u_{j-1}^n}{2}}{\Delta T} + \frac{f(u_{j+1}^n) - f(u_{j-1}^n)}{2\Delta x} = 0 \quad (\text{B.4})$$

It can be shown that this scheme is stable<sup>2</sup>. Rearranging the different terms, we can write the scheme in *conservative form*:

$$u_j^{n+1} = u_j^n - \frac{\Delta t}{\Delta x} \left( F_{j+1/2}^n - F_{j-1/2}^n \right) \quad (\text{B.5})$$

with

$$F_{j+1/2}^n = \frac{1}{2} (f(u_{j+1}^n) + f(u_j^n)) - \frac{1}{2} \frac{\Delta x}{\Delta t} (u_{j+1}^n - u_{j-1}^n) \quad (\text{B.6})$$

The numerical fluxes  $F_{j+1/2}^n$  and  $F_{j-1/2}^n$  are numerical approximations of the real flux of  $u$  at the edges of cell number  $j$ . The Lax and Friedrichs scheme is only first-order accurate. To have a better accuracy, one can find better numerical approximations  $F_{j\pm 1/2}^n$  of the flux.

## B.3 The Kurganov and Tadmor scheme

The scheme elaborated by Kurganov and Tadmor (cf [6]) can be seen as a modified version of the Lax and Friedrichs scheme approximating better the flux function. The idea is to evaluate numerically the value of  $u$  at the edges of the cell to gain accuracy. For example the value at the right edge of cell number  $j$ , which we call  $u_{j+1/2}^n$  according to our notation, will be computed using

$$u_{j+1/2}^n = u_j^n + \frac{\Delta X}{2} \frac{\partial}{\partial x} u_j^n \quad (\text{B.7})$$

where the partial derivative is computed using a finite difference formula. Note that unless our finite differences are perfectly accurate,  $u_{j+1/2}^n \neq u_{(j+1)-1/2}^n$ <sup>1</sup>! The numerical flux is now

$$F_{j+1/2}^n = \frac{1}{2} \left( f(u_{j+1/2}^n) + f(u_{(j+1)-1/2}^n) \right) - \frac{1}{2} |a_{j+1/2}^n| (u_{(j+1)-1/2}^n - u_{j+1/2}^n) \quad (\text{B.8})$$

Note that the term  $\Delta x / \Delta t$  has been replaced by the local advection speed  $|a_{j+1/2}^n|$ . This also plays a key role in ensuring the accuracy of the scheme.

---

edge.

2. If the so-called Courant-Friedrich-Levy condition is satisfied. Essentially, the ratio of the spatial and temporal discretisation  $\Delta x / \Delta t$  must be chosen greater than the local advection speed.

The Kurganov and Tadmor scheme is remarkably simple, accurate and stable. If we chose a correct finite difference formula to compute the derivatives appearing in the edges values of  $u$ , the scheme can be shown to be second order accurate. That means that shocks, frequently appearing in the solutions of conservation laws, will be well resolved. It also exhibits the important *total variation diminishing property*, which ensures that no oscillations will appear near the shocks.

# Appendix C

# Programming

In this appendix, I briefly present the code I developed during this internship. The program was done in `C++`. As object-oriented programming is extensively used, rather than giving the code detailed working scheme, I will sum up its class structure. The entire code source is available here: [https://github.com/Yukee/flume/tree/3D/KT\\_solver](https://github.com/Yukee/flume/tree/3D/KT_solver).

## C.1 Containers

Numerical data and equations are stored in objects called *containers*.

### C.1.1 Scalar fields

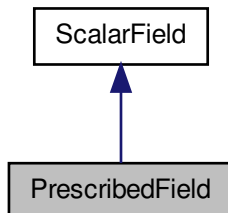


Figure C.1

Numerical data is stored in objects of the `PrescribedField` class. This class derives from the `ScalarField` class. A `ScalarField` object represents a scalar field sampled on a discrete grid. Two such object can be added, multiplied the same way scalar fields can. `ScalarField` are used for example to store the concentration,  $\phi$ , sampled on the integration grid. `PrescribedField` objects are derived from `ScalarField`. In addition to behaving as scalar fields, `PrescribedField` objects can store informations about the boundary conditions at the surface bounding the domain of definition of the scalar field. One can *prescribe* the value of the field (Dirichlet boundary condition) or the value of its derivative normal to the surface (Von Neumann boundary condition).

For testing purposes, I also used `PeriodicField` objects, behaving like scalar fields with periodic boundary conditions.

### C.1.2 Flux functions

`Flux` objects behave like functions. They are used to store the information about what is the flux function  $f$  (cf appendix B for the definition) in the conservation law we want to solve. If we want to

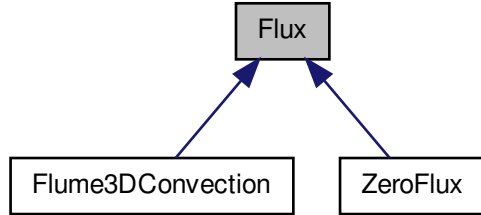


Figure C.2

construct a new flux function, we just have to derive the base class (figure C.2).

### C.1.3 Equations

`Equation` objects are used to store informations about the equation we want to solve numerically, namely

$$\frac{\partial}{\partial t}\phi + \frac{\partial}{\partial x}f(\phi, x) = \frac{\partial}{\partial x}D\left(\phi, \frac{\partial\phi}{\partial x}\right) + S(\phi, x) \quad (\text{C.1})$$

An `Equation` stores the form of the advection flux  $f$ , of the diffusion flux  $D$  and of the source term  $S$  in `Flux` objects.

Note that this equation is slightly different from a conservation law, because of the addition of the source term  $S$  and the diffusion term  $D$ , but it can be solved in the same way. A source term appear for example when we solve the 2D segregation equation in the centre plane, as explained in chapter 2. A diffusion flux will appear if we wish to model the effect of viscosity on the granular flow. It was not used during the internship, but can be handled by the program, and may be used in the future.

## C.2 Solvers

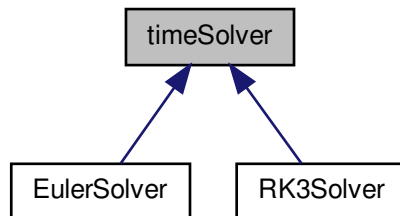


Figure C.3

Solvers are objects designed to integrate the above equation. To do the time evolution, the `timeSolver` calls repetitively the `KTSolver`, whose role is to compute the numerical fluxes at the edges of the cells (cf appendix B).

For time stepping, we used the simple Euler method, and the more sophisticated order three Runge-Kutta method. If we want to construct a new method, we just have to derive the `timeSolver` class.

I would like to insist on the fact that the program is very general. It is able to solve any system of laws of the type (1.1), in any number of spatial dimensions.

### C.3 Another approach

At the end of my internship, I created a new code based on a totally different approach. The base container of this new code was the `Cell`. A `Cell` object represent a finite volume cell (cf appendix ??). It contains the value of the solved field, and the values of the numerical fluxes at its edges. A `CellArray` object stores the cells forming the integration domain.

This approach is powerful, especially for handling boundary conditions. for example, if we want to prescribe the flux to be zero at the boundary of the domain, we just have to create a new class `BoundaryCell` derived from `Cell`, and taking into account this specificity. The `CellArray` object will then contain an heterogeneous collection of `Cell` objects (forming the inner part of the integration domain) and `BoundaryCell` objects (forming the boundary of the integration domain).

Using this approach, it is also very easy to use different numerical schemes to integrate the differential equation. I was thus able to test a number of different approaches. The source code is available here: [https://github.com/Yukee/finite-volume/tree/master/KT\\_new\\_1D](https://github.com/Yukee/finite-volume/tree/master/KT_new_1D).

# Appendix D

## Method of characteristics

In this appendix, we present a general method to solve *hyperbolic partial differential equations*, a class of equations to which conservation laws belong. We believe it is best to see the method in action with an example. As we are interested in solving segregation equations, in this appendix we will solve a simplified version of the fully 3D segregation equation:

$$u(z) \frac{\partial}{\partial x} \phi - q \frac{\partial}{\partial z} \phi (1 - \phi) = 0 \quad (\text{D.1})$$

This is the 2D version of our equation, in the stationary regime, and for the most simple velocity profile:

$$\mathbf{v} = \begin{pmatrix} u \\ 0 \end{pmatrix} \quad (\text{D.2})$$

In this case, since we assume incompressibility,  $u$  is a function of  $z$  only.

### D.1 Characteristic curves

The steady-state solution is a function of 2 variables:  $\phi = \phi(x, z)$ . So the solution can be seen as the surface  $\phi - \phi(x, z) = 0$  of the 3D space  $(x, z, \phi)$ . *Characteristics* are curves defined by  $\phi = \Phi(x(s), z(s))$  lying on the solution surface, and satisfying

$$\frac{d\Phi}{ds} = 0 \quad (\text{D.3})$$

Using chain rule we have

$$\frac{dx}{ds} \frac{\partial \Phi}{\partial x} + \frac{dz}{ds} \frac{\partial \Phi}{\partial z} = 0 \quad (\text{D.4})$$

and since  $\Phi$  is lying on the solution surface,

$$\frac{dx}{ds} = u \quad (\text{D.5})$$

$$\frac{dz}{ds} = -q(1 - 2\Phi) \quad (\text{D.6})$$

So solving the segregation equation (and in fact, any conservation law) is equivalent to solving a system of ordinary differential equations, which is easier to do. Indeed we have at our disposal a number of tools to attack ordinary differential equations, whereas very few will work with partial differential equations such as conservation laws.

Rather than using a parameter  $s$ , we can directly express  $z$  as a function of  $x$ , and since

$$\frac{dz}{ds} = \frac{dx}{ds} \frac{dz}{dx} \quad (\text{D.7})$$

we have

$$u \frac{dz}{dx} = -q(1 - 2\Phi) \quad (\text{D.8})$$

This equation is known as the characteristic equation, because solving it will give us the equation of any characteristic curve lying on the solution surface. This is then sufficient to reconstruct the whole solution.

## D.2 Change of coordinates

Of course, to solve the characteristic equation in our case, we need to know the explicit expression of the velocity  $u$ . But there is a clever way to get around this difficulty. We note that since the flow is *incompressible*, we can define the stream function  $\psi$  as

$$\frac{\partial \psi}{\partial x} = -w \quad (\text{D.9})$$

$$\frac{\partial \psi}{\partial z} = u \quad (\text{D.10})$$

In our case of course  $w$  is zero, but this method is more general.

Now we remap the  $z$  axis of the physical space using  $\psi$ . We make the change of coordinate  $z \leftarrow \psi$ . For example, let us choose a simple linear velocity profile:

$$u(z) = \frac{U}{H} \left( z - \frac{H}{2} \right) \quad (\text{D.11})$$

with  $z$  varying from 0 to  $H$ . The stream function is then

$$\psi(z) = \frac{U}{2H} \left( z - \frac{H}{2} \right)^2 \quad (\text{D.12})$$

Note that  $\psi$  takes the same value for 2 different values of  $z$ :  $\psi(z) = \psi(H-z)$ . In other words,  $z \rightarrow \psi(z)$  is not a bijection (and therefore not a good change of coordinates) on the interval  $[0, H]$ . But this is not a problem, it just means that we need to cut our interval by the middle, and solve separately for each half.

Back to the general solving of the characteristic equation, if we make the change of coordinates, we have using chain rule again,

$$u \frac{dz}{dx} = \frac{\partial \psi}{\partial z} \frac{dz}{dx} = \frac{d\psi}{dz} \quad (\text{D.13})$$

so, in the new system of coordinates, we can solve for the characteristic curves without knowing explicitly the velocity field! Indeed now we have

$$\frac{d\psi}{dz} = -q(1 - 2\Phi) \quad (\text{D.14})$$

and since  $\Phi$  is constant along the characteristic curve,

$$\psi(x) = -qx(1 - 2\Phi) + \psi_0 \quad (\text{D.15})$$

And that is it! We just solved our problem. Of course it is just a trick: the velocity profile explicit dependence is hidden in  $\psi$ , as we need to know it to actually do the change of coordinate. But this trick is exceedingly useful to understand the global structure of the solution without having to prescribe a velocity field, as we will see now.

## D.3 Shock waves and jump condition

We said that we can decompose our surface solution as a set of curves, called characteristic curves. This is the essence of the method of characteristics. What happens if two such curves cross? In that case the method can no longer be used, and in fact the solution is no longer a function, but becomes a discontinuous *distribution*.

In the physical space  $(x, z)$  two regions where the solution  $\psi$  is a function are separated by a discontinuity in  $\psi$ , a *jump* in the concentration. The equation of the interface can be calculated using the so-called Rankine-Hugoniot jump condition. We will not give here a demonstration of this formula as the derivation in itself is not specially enlightening, but I can be found for example in [8].

In our case, the condition is

$$\frac{d\psi}{dx} = q(\phi^+ + \phi^- - 1) \quad (\text{D.16})$$

where  $\phi^+$  and  $\phi^-$  are the concentrations at each side of the interface.

This jump condition and the characteristic equation is all we need to know to understand the full structure of the solution. But of course, we need to prescribe a boundary condition to start with.

## D.4 Structure of the solution

We will solve our equation on a bounded domain. We won't give any details on the chosen velocity profile. We will just prescribe the value of the  $\phi$  at the left boundary of our domain. Let us suppose it is a constant (ie we start with an homogeneous mixture of small and large particles) and call it  $\phi_0$ . The particles will be advected to the right by the velocity field, and the concentration will evolve as  $x$  increases.

How? Well, we know from experiments and from our intuition that after some time (ie from  $x$  sufficiently large) the mixture will be fully segregated, ie a jump will separate a region of large particles ( $\phi = 0$ ) and a region of small particles ( $\phi = 1$ ). Similarly, the initial region of concentration  $\phi_0$  will be separated from the upper region of large particles by a jump. If we use the jump condition, with  $\phi^- = \phi_0$  and  $\phi^+ = 0$ , we have

$$\psi^u(x) = \psi_0^u - qx(1 - \phi_0) \quad (\text{D.17})$$

similarly, for the jump separating the lower region of small particles ( $\phi^+ = 1$ ) and the homogeneous region ( $\phi^- = \phi_0$ ),

$$\psi^l(x) = qx\phi_0 \quad (\text{D.18})$$

These two shocks will begin immediately to form, at  $x = 0$ . They will join at some point called the triple point, because it is at the interface between 3 regions: the homogeneous region, the large particles region and the small particles region. The whole structure is summed up in the figure D.1.

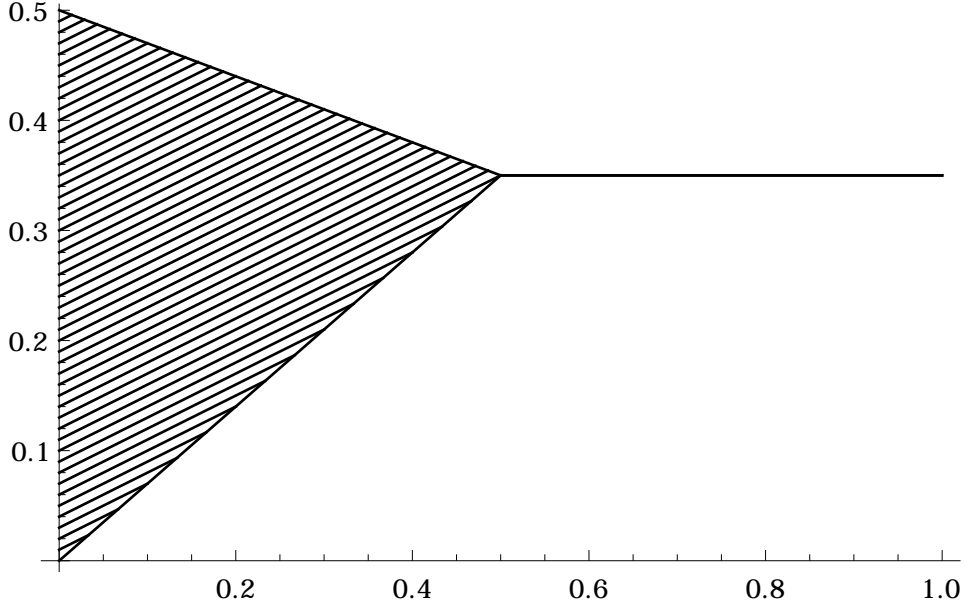


Figure D.1: Structure of the solution of the simplified segregation equation, with an homogeneous concentration input. The characteristics are shown, as well as the jumps (in bold).

# Bibliography

- [1] K. O. Friedrichs and P. D. Lax. Boundary value problems for first order operators. *Communications on Pure and Applied Mathematics*, 18(1-2):355–388, 1965.
- [2] J. M. N. T. Gray and C. Ancey. Segregation, recirculation and deposition of coarse particles near two-dimensional avalanche fronts. *Journal of Fluid Mechanics*, 629:387–423, 6 2009.
- [3] J. M. N. T. Gray and L. W. Morland. A two-dimensional model for the dynamics of sea ice. *Philosophical Transactions of the Royal Society of London. Series A: Physical and Engineering Sciences*, 347(1682):219–290, 1994.
- [4] C. G. Johnson, B. P. Kokelaar, R. M. Iverson, M. Logan, R. G. LaHusen, and J. M. N. T. Gray. Grain-size segregation and levee formation in geophysical mass flows. *Journal of Geophysical Research: Earth Surface*, 117(F1):n/a–n/a, 2012.
- [5] P. Jop, Y. Forterre, and O. Pouliquen. A constitutive law for dense granular flows. *Nature*, 441:727–730, 2006.
- [6] Alexander Kurganov and Eitan Tadmor. New high-resolution central schemes for nonlinear conservation laws and convection-diffusion equations. *J. Comput. Phys.*, 160:241–282.
- [7] Peter Lax and Burton Wendroff. Systems of conservation laws. *Communications on Pure and Applied Mathematics*, 13(2):217–237, 1960.
- [8] Randall J. Leveque. *Finite Volume Methods for Hyperbolic Problems*. Cambridge University Press, 2002.
- [9] GDR MiDi. On dense granular flows. *Eur. Phys. J. E*, 14:341–365, 2004.
- [10] O. Pouliquen. Scaling laws in granular flows down rough inclined planes. *Physics of Fluids*, 11(3):542–548, 1999.
- [11] A. Thornton, J. M. N. T. Gray, and A. J. Hogg. A three-phase mixture theory for particle size segregation in shallow granular free-surface flows. *Journal of Fluid Mechanics*, 550:1–25, 2006.